Materials Letters (2013). 98, 182-185.
DOI: http://dx.doi.org/10.1016/j.matlet.2013.02.052

The microstructural evolution of a pre-alloyed AZ91 magnesium alloy powder through high-energy milling and subsequent isothermal annealing

M.A. Jabbari Taleghani [a,b,*], J.M. Torralba [a,b]

[a] *Department of Materials Science and Engineering, Universidad Carlos III de Madrid, Avenida de la Universidad 30, 28911 Leganés, Madrid, Spain*
[b] *IMDEA Materials Institute, C/Eric Kandel 2, Tecnogetafe, 28906 Getafe, Madrid, Spain*

Corresponding author at: IMDEA Materials Institute, C/Eric Kandel 2, Tecnogetafe, 28906 Getafe, Madrid, Spain. Tel.: +34 91 5493422; fax: +34 91 5503047.
**E-mail addresses:* mohammad.jabbari@imdea.org, mo.jabbari@yahoo.com (M.A.J. Taleghani).

Abstract: This study analyzed the effect of high-energy milling (HEM) and subsequent isothermal annealing on the microstructural characteristics of a pre-alloyed AZ91 Mg alloy powder. To this end, the mentioned powder was milled for 14 h using a horizontal attritor. Then, the mechanically milled powder was isothermally annealed at temperatures ranging from 200 °C to 500 °C for 1 h up to 4 h in an Ar atmosphere. HEM caused the β-$Mg_{17}Al_{12}$ phase present in the microstructure of AZ91 powder particles to dissolve into their α-Mg solid solution matrix. In addition, the crystallite size of the α-Mg phase decreased to 25 nm through HEM. In contrast to the annealing time, the temperature of isothermal annealing had a significant effect on the microstructural features of the mechanically milled AZ91 powder.

Keywords: AZ91 magnesium alloy, Pre-alloyed powder, High-energy milling, Isothermal annealing, Microstructural evolution

1. Introduction

Mg alloys have received considerable attention as a structural material in recent years due to their interesting properties, such as low density, high strength-to-weight ratio, good damping characteristics, superior machinability, and excellent castability [1]. Most of the research and development on Mg alloys has been performed by the automotive industry; and die casting has been the main manufacturing route for Mg products because of the poor workability of Mg at room temperature, which is a result of its HCP crystal structure [2,3].

Although the market for Mg products continues to grow, many opportunities remain untapped because of the low stiffness and strength of Mg alloys [4]. Due to the limited number of slip systems of Mg and its correspondingly large Taylor factor, grain refinement remarkably improves the mechanical properties of Mg and its alloys. It is well known that the fine-grained Mg alloys exhibit an interesting combination of high strength and high ductility at room temperature and superplasticity at elevated temperatures [5,6].

In the 1960s, high-energy milling (HEM) was first developed by Benjamin and his co-workers to fabricate oxide-dispersion-strengthened (ODS) nickel-based superalloys [7]. In recent years, this technique has been widely exploited for the production of nanostructured materials. Grain sizes with nanometer dimensions have been observed in almost all mechanically milled pure metals, alloys, and intermetallics [8,9].

Although the processing of nanostructured light materials, such as Al alloys and composites, by HEM has been the subject of many studies [10–12], studies on the HEM of Mg and its alloys are scarce. However, processing by HEM also has considerable potential for Mg alloys because fine-grained Mg alloys have a unique combination of properties. Among all of the existing Mg alloys, AZ91 is the most widely used alloy in industry [13]. Therefore, this study focused on the fabrication of a nanostructured AZ91 Mg alloy by HEM. Furthermore, as the mechanically milled powders are then consolidated by powder metallurgy (PM) routes, such as cold pressing and sintering, powder extrusion, powder forging, and powder rolling, the microstructural evolution of the milled AZ91 powder during subsequent consolidation processes at high temperatures was also studied by isothermal annealing at different temperatures.

2. Materials and methods

The raw material used for this study was a pre-alloyed Mg–Al–Zn powder (Ecka Granules, Germany) with a chemical composition equivalent to that of AZ91 D alloy (8.8 wt% Al, 0.6 wt% Zn, 0.2 wt% Mn, 0.03 wt% Si, and the balance Mg). The above-mentioned powder was milled in a horizontal attritor (CM01 Simoloyer, ZOZ, Germany) using the following milling parameters: ball-to-powder weight ratio—20/1; ball diameter—5 mm; ball material—AISI 420 stainless

steel; milling time—14 h; milling speed—700 rpm; and milling atmosphere—Ar. Stearic acid (2 wt%) was also employed as the process control agent (PCA). Special precautions should be taken during unloading of the Mg-based powders after HEM. Immediately after milling, the milled powder is hot (or at least warm) and therefore the lid should not be immediately opened. Furthermore, after opening the lid and prior to unloading, the milled powder must be exposed to atmosphere for a couple of hours. Otherwise, the powder may catch fire during unloading because of interaction with the oxygen. The isothermal annealing of the mechanically milled AZ91 (MM AZ91) powder was then performed at annealing temperatures of 200 °C, 300 °C, 400 °C, and 500 °C for annealing times of up to 4 h in an Ar atmosphere.

The microstructural evolution and phase changes of AZ91 powder through HEM and subsequence isothermal annealing were studied by X-ray diffractometry (XRD). In addition, the crystallite size of the α-Mg solid solution matrix of MM AZ91 powder particles was determined from the broadening of XRD peaks using the Williamson–Hall method.

3. Results and discussion

Mechanical milling: The particles of AZ91 powder possessed an irregular, flake-like morphology (Fig. 1(a)) with an average particle size of 105 μm and a very broad size distribution ($D_{0.9}$–$D_{0.1}$ = 183 μm). This morphology is typical of Mg-based powders produced by the mechanical grinding of casting ingots.

The MM AZ91 powder (Fig. 1(b)) exhibited an equiaxed morphology, which implies that the employed milling time, i.e. 14 h, was sufficient for the milling process to reach its steady state, in which there is a balance between the cold welding and fracturing of powder particles. The average particle size and size distribution ($D_{0.9}$–$D_{0.1}$) of MM AZ91 powder were measured to be 37 μm and 100 μm, respectively, suggesting that the milling process had a remarkable effect on the particle size characteristics of AZ91 powder.

The XRD patterns of AZ91 and MM AZ91 powders are presented in Fig. 2. The microstructure of the AZ91 powder particles was composed of the β-$Mg_{17}Al_{12}$ precipitates and the α-Mg solid solution matrix. This structure is typical of AZ91 castings [14]. HEM remarkably affected the intensities and widths of the diffraction peaks of the α-Mg phase, and the mentioned peaks became weaker and wider through HEM. This phenomenon can be attributed to the reduction in particle size, the refinement of crystallite size, and the enhancement of lattice strain, all promoted by the severe plastic deformation of the AZ91 powder particles during HEM. Moreover, the diffraction peaks of the β-$Mg_{17}Al_{12}$ phase are barely detectable in the XRD pattern of MM AZ91 powder, which can be related to the dissolution of the β-$Mg_{17}Al_{12}$ phase in the α-Mg matrix of the powder particles. Another possibility is that HEM caused the β-$Mg_{17}Al_{12}$ phase to be refined into very small dispersoids distributed in the α-Mg phase, which are hardly detectable by XRD. The grain sizes of AZ91 casting products normally range between 10 μm and 150 μm [14,15]. The AZ91 powder used for this study had been produced by the mechanical grinding of AZ91 casting ingots. Considering the production method and the average particle size of the employed AZ91 powder (105 μm), it can be concluded that the grains of this powder should have had micrometer dimensions. The crystallite size and lattice strain of MM AZ91 powder were calculated to be 25 nm and 0.53%. A high lattice strain implies that the AZ91 powder particles went through severe plastic deformation during the HEM process and, as a result, contained a high density of microstructural defects. The values obtained for crystallite size and lattice strain are in good agreement with those previously reported for high-energy milled Al-based powders [10,16]. Various models have been proposed to describe the mechanism of formation of nanostructures by HEM [9].

Isothermal annealing: The XRD patterns of MM AZ91 powder annealed for 1 h at 200 °C, 300 °C, 400 °C, and 500 °C are shown in Fig. 3(a). The displacement of the α-Mg (101) diffraction peak through the annealing of MM AZ91 powder at the above-mentioned temperatures is also illustrated in Fig. 3(b). As shown in Fig. 3, annealing at 200 °C for 1 h boosted the diffraction peaks of the β-$Mg_{17}Al_{12}$ phase in the XRD pattern of MM AZ91 powder

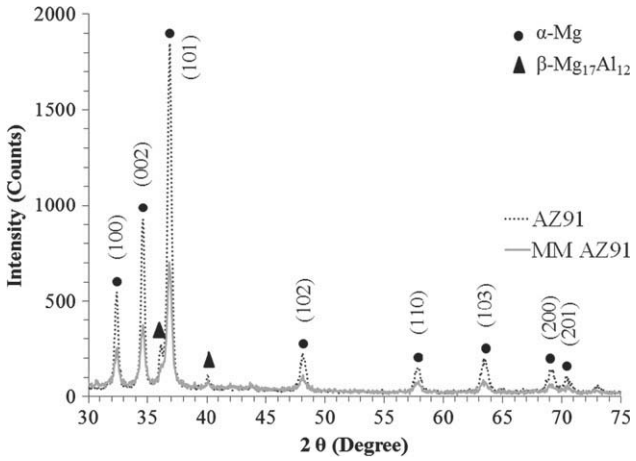

Fig. 2. The XRD patterns of AZ91 (dotted) and MM AZ91 (solid) powders.

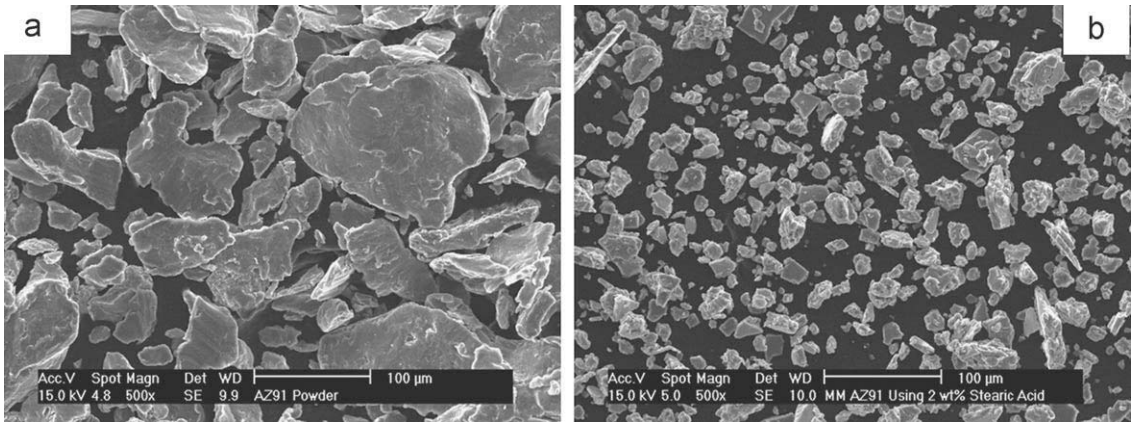

Fig. 1. The morphologies of (a) AZ91 and (b) MM AZ91 powders.

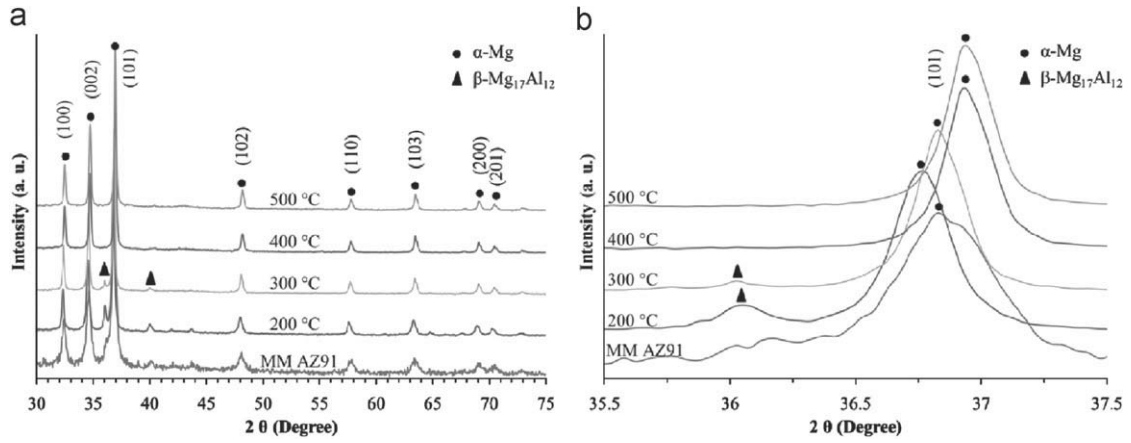

Fig. 3. (a) The XRD patterns of MM AZ91 powder annealed at different temperatures for 1 h and (b) the displacement of the α-Mg (101) diffraction peak.

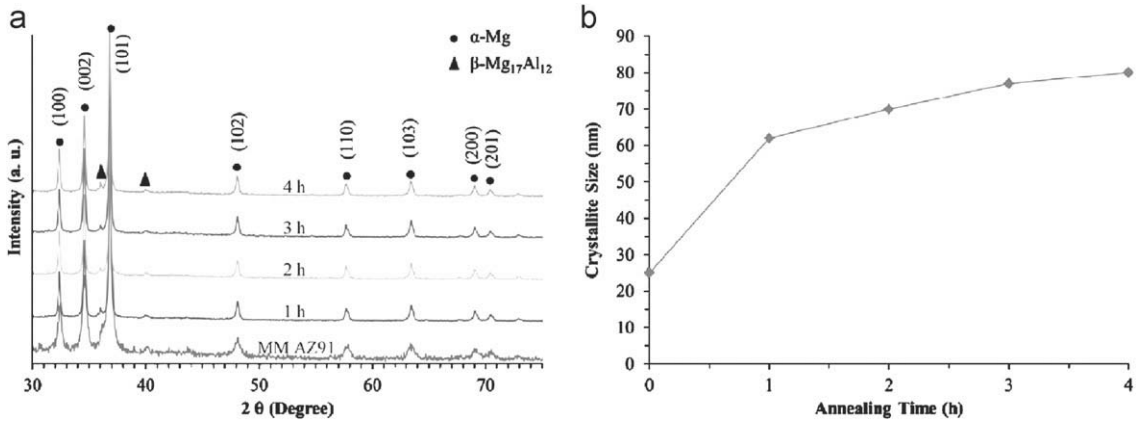

Fig. 4. (a) The XRD patterns and (b) the crystallite sizes of MM AZ91 powder annealed at 300 °C for different times.

and caused the α-Mg (101) peak to shift to a lower diffraction angle, which can be attributed to the rejection of Al atoms by the supersaturated α-Mg solid solution matrix of MM AZ91 powder particles and the formation and growth of β-$Mg_{17}Al_{12}$ precipitates. However, as the annealing temperature increased from 200 °C to 300 °C, the intensities of the diffraction peaks of the β-$Mg_{17}Al_{12}$ phase decreased, and the α-Mg (101) peak shifted nearly to its initial diffraction angle, which can be related to an increase in the solubility of Al atoms in the α-Mg phase at this temperature. At annealing temperatures of 400 °C and 500 °C, the diffraction peaks of the β-$Mg_{17}Al_{12}$ phase disappeared, and the α-Mg (101) peak shifted to higher diffraction angles, showing the complete dissolution of the β-$Mg_{17}Al_{12}$ phase in the α-Mg matrix of the AZ91 powder particles. To dissolve the β-$Mg_{17}Al_{12}$ precipitates in the α-Mg matrix, the AZ91 cast products are normally annealed and homogenized at 415 °C for 12–24 h [14]. Nevertheless, annealing times as short as 1 h were enough to completely dissolve the β-$Mg_{17}Al_{12}$ phase in the α-Mg matrix of MM AZ91 powder particles, which suggests a very high diffusion rate for Al atoms in the α-Mg phase. Moreover, the accelerated dissolution of β-$Mg_{17}Al_{12}$ phase for MM AZ91 powder can also be attributed to the fact that the β-$Mg_{17}Al_{12}$ precipitates dispersed in the microstructure of MM AZ91 powder particles are significantly smaller than those normally found in the microstructure of AZ91 cast products.

The XRD patterns of MM AZ91 powder annealed at 300 °C for 1–4 h are illustrated in Fig. 4(a), showing that all of the microstructural changes for MM AZ91 powder occurred in the first hour of annealing, after which no significant microstructural change was detectable. This can be attributed to the high diffusion rates of alloying elements in the α-Mg solid solution matrix of MM AZ91 powder particles, promoted by the high density of structural defects and grain boundaries present in the microstructure of MM AZ91 powder particles.

The crystallite size of MM AZ91 powder annealed at 300 °C for 4 h was determined to be 80 nm (Fig. 4(b)), suggesting that the nanostructured AZ91 alloy processed by HEM had a good thermal stability. This favorable thermal stability could result from the homogenous distribution of nanosized Mg oxides and carbides in the structure of MM AZ91 powder particles. The surfaces of Mg-based powders are covered with a thin, stable oxide layer of 3–5 nm [17], which can be fragmented and introduced into the structure of powder particles by HEM. Moreover, Mg may react with PCA and form nanosized Mg carbides during HEM. LECO measurements confirmed that the oxygen and carbon content of AZ91 powder increased from 0.015 wt% and 0.012 wt%, respectively, to 0.045 wt% and 1.52 wt% through mechanical milling. The growth of MM AZ91 grains at high temperatures can then be hindered by the Mg oxide and carbide dispersoids.

4. Conclusions

This study investigated the morphological and microstructural evolution of a pre-alloyed AZ91 powder through HEM and subsequent isothermal annealing. The milling process significantly changed the morphology and size distribution of the AZ91 powder. In addition, the microstructure of the AZ91 powder

was remarkably refined by HEM. The annealing of MM AZ91 powder at temperatures less than or equal to 300 °C boosted the intensities of the diffraction peaks of the β-$Mg_{17}Al_{12}$ phase. However, annealing at 400 °C for 1 h was sufficient for the complete dissolution of β-$Mg_{17}Al_{12}$ precipitates in the α-Mg matrix of MM AZ91 powder particles. The nanostructured AZ91 alloy processed by HEM showed a good thermal stability, retaining its crystallite size of less than 100 nm after the annealing of MM AZ91 powder at 300 °C for 4 h.

Acknowledgment

The authors would like to thank the Comunidad de Madrid for their financial support of this work through the ESTRUMAT Grant #S2009/MAT-1585.

References

[1] Volkova E. Modern magnesium-base deformable alloys and composite materials (a review). Met Sci Heat Treat 2006;48:473–8.
[2] Kulekci M. Magnesium and its alloys applications in automotive industry. Int J Adv Manuf Technol 2008;39:851–65.
[3] Liang SJ, Liu ZY, Wang ED. Microstructure and mechanical properties of Mg–Al–Zn alloy deformed by cold extrusion. Mater Lett 2008;62:3051–4.
[4] Li L, Lai MO, Gupta M, Chua BW, Osman A. Improvement of microstructure and mechanical properties of AZ91/SiC composite by mechanical alloying. J Mater Sci 2000;35:5553–61.
[5] Kubota K, Mabuchi M, Higashi K. Review processing and mechanical properties of fine-grained magnesium alloys. J Mater Sci 1999;34:2255–62.
[6] Li Y, Chen Y, Cui H, Ding J, Zuo L, Zhang J. Hot deformation behavior of a spray-deposited AZ31 magnesium alloy. Rare Met 2009;28:91–7.
[7] Benjamin J. Dispersion strengthened superalloys by mechanical alloying. Metall Mater Trans B 1970;1:2943–51.
[8] Adamiak M, Fogagnolo JB, Ruiz-Navas EM, Dobrzañski LA, Torralba JM. Mechanically milled AA6061/(Ti3Al)P MMC reinforced with intermetallics—the structure and properties. J Mater Process Technol 2004;155–156:2002–6.
[9] Suryanarayana C. Mechanical alloying and milling. Prog Mater Sci 2001;46:1–184.
[10] Fogagnolo JB, Robert MH, Torralba JM. Mechanically alloyed AlN particle-reinforced Al-6061 matrix composites: powder processing, consolidation and mechanical strength and hardness of the as-extruded materials. Mater Sci Eng A 2006;426:85–94.
[11] Tavoosi M, Karimzadeh F, Enayati MH. Fabrication of Al–Zn/α-Al_2O_3 nanocomposite by mechanical alloying. Mater Lett 2008;62:282–5.
[12] Manna I, Chattopadhyay PP, Banhart F, Fecht HJ. Solid state synthesis of amorphous and/or nanocrystalline Al40Zr40Si20 alloy by mechanical alloying. Mater Lett 2004;58:403–7.
[13] Ishikawa K, Watanabe H, Mukai T. High strain rate deformation behavior of an AZ91 magnesium alloy at elevated temperatures. Mater Lett 2005;59:1511–5.
[14] Li J-y, Xie J-x, Jin J-b, Wang Z-x. Microstructural evolution of AZ91 magnesium alloy during extrusion and heat treatment. Trans Nonferrous Met Soc China 2012;22:1028–34.
[15] Cerri E, Leo P, De Marco PP. Hot compression behavior of the AZ91 magnesium alloy produced by high pressure die casting. J Mater Process Technol 2007;189:97–106.
[16] Yazdian N, Karimzadeh F, Tavoosi M. Microstructural evolution of nanostructure 7075 aluminum alloy during isothermal annealing. J Alloys Compd 2010;493:137–41.
[17] Wolff M, Ebel T, Dahms M. Sintering of magnesium. Adv Eng Mater 2010;12:829–36.